



Enhanced lateral photovoltaic effect in 3C-SiC/Si heterojunction under external electric field

Tuan-Hung Nguyen^{a,*}, Trung-Hieu Vu^a, Tuan Anh Pham^a, Dinh Gia Ninh^a,
 Cong Thanh Nguyen^a, Hong-Quan Nguyen^a, Braiden Tong^a, Dang D.H. Tran^a, Erik W. Streed^{b,c},
 Van Thanh Dau^d, Nam-Trung Nguyen^a, Dzung Viet Dao^{a,d}

^a Queensland Micro and Nanotechnology Centre, Griffith University, Nathan, QLD 4111, Australia

^b Institute for Glycomics, Griffith University, 1 Parkland Dr, Southport, QLD 4215, Australia

^c Centre for Quantum Dynamics, Griffith University, Nathan, QLD 4111, Australia

^d School of Engineering and Built Environment, Griffith University, 1 Parkland Dr, Southport, QLD 4215, Australia

ARTICLE INFO

Keywords:

Lateral photovoltaic effect
 Position-sensitive detector
 3C-SiC/Si
 Sensor

ABSTRACT

Position-sensitive detector (PSD) is a popular type of noncontact optical position sensor that has important roles in various applications. Cubic-silicon carbide on silicon (3C-SiC/Si) is a promising platform to develop optoelectronic sensors for harsh environment applications thanks to the superior robustness of the SiC, the low wafer cost, and the high compatibility with the well-established Si micro/nano fabrication technology. Here, we report an enhanced lateral photovoltaic effect (LPE) in 3C-SiC/Si heterojunction under an external electric field, and demonstrate the effect in an ultrasensitive PSD. We observed a position sensitivity of 1550 mV/mm, which is a five-time increase compared to the case without electric field. The generation and transport of the photo-induced charge carriers are investigated by examining the band diagram of the 3C-SiC/Si heterojunction to provide a detail explanation of the phenomenon. Our findings in this work demonstrate the potential of the 3C-SiC/Si heterojunction to develop high-performance noncontact optical sensors for harsh environment applications.

1. Introduction

Optical sensing technologies are an important topic that has been extensively reported with various implementations in commercial electronics, industry, and military/defence [1–4]. PSDs are among the most crucial class of optical sensors that have been employed in a broad variety of applications including motion tracking, atomic force microscopy, and angular displacement monitoring [5–9]. A traditional type of PSD is the quadrant detector (QD) which consists of four discrete photodiodes and the position of the light spot can be derived from the ratio of the outputs from each photodiode [10,11]. For applications that require higher sensitivity, the LPE detector is utilised [12–14]. The LPE detector consists of a single photodiode with two or four contacts and the output voltage between two contacts depends on the relative position of the light spot with the contacts. In contrast to the QD, the LPE detector can provide continuous data with high resolution, sensitivity, and fast response time. The PSDs based on the LPE have advanced dramatically over the last two decades with multiple publications on ultrasensitive PSDs [15–18]. A wide range of materials has been explored to develop high-performance PSDs [19–26]. Notably,

introducing an external modulation has been known to be an effective method to improve the performance of PSDs. Zheng et al. reported an enhanced LPE in WS₂/Si structure using ferroelectrics [27]. By applying a ferroelectric gate, the absorption wavelength of the structure was broadened to infrared range (405–1550 nm). The position sensitivity also increased from 198.6 mV/mm to 503.2 mV/mm. In addition, the response speed of the WS₂/Si structure also improved significantly due to a higher carrier initial kinetic energy. Liu et al. also reported a PSD in Cu(In, Ga)Se₂ (CIGS) multi-layer heterostructure, tuned by piezopyroelectric effect [28]. Due to the coupling between piezoelectric and pyroelectric effect, the position sensitivity of the heterostructure can be enhanced by 171.8%, up to 639.9 mV/mm. The response time was also reduced to 6.8/7.9 μs.

Silicon (Si) is the material of choice for microelectronics due to its abundance, low cost, and most importantly, well-established micro/nano fabrication technology. The indirect bandgap and narrow absorption band of Si, however, impede the development of Si optoelectronics. Moreover, Si is unsuited for applications in harsh environments

* Corresponding author.

E-mail addresses: hung.nguyen@griffith.edu.au (T.-H. Nguyen), d.dao@griffith.edu.au (D.V. Dao).

<https://doi.org/10.1016/j.sna.2023.114746>

Received 30 March 2023; Received in revised form 1 August 2023; Accepted 10 October 2023

Available online 13 October 2023

0924-4247/© 2023 The Author(s). Published by Elsevier B.V. This is an open access article under the CC BY license (<http://creativecommons.org/licenses/by/4.0/>).

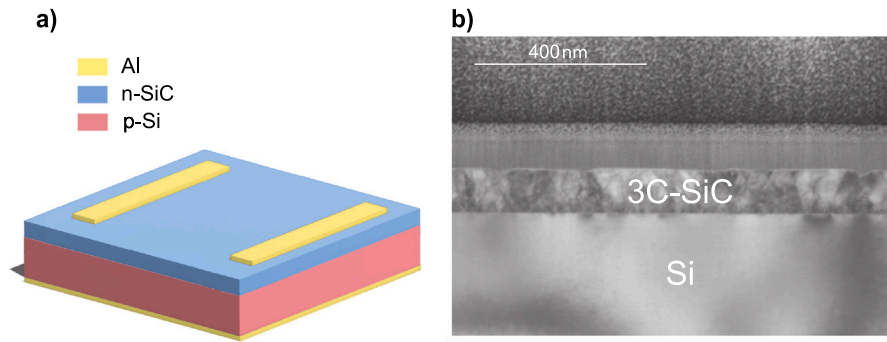


Fig. 1. (a) n-3C-SiC/p-Si heterojunction device structure. (b) TEM image of the heterojunction.
Source: Reprinted with permission from [29].
© 2023 IEEE.

such as chemically corrosive environments. To overcome this limitation, heterostructures are used to improve the performance and sensitivity of the device by combining the unique properties of different materials. A larger number of reports on LPE detectors utilises heterostructures of Si and other materials [27,30–35]. High sensitivity, fast response time and wide spectral range were demonstrated on a variety of heterostructure devices. SiC with its excellent mechanical, electrical, and thermal properties and chemical inertness is a material that can complement or potentially replace Si, especially in harsh environment applications [36,37]. Among the polytypes, cubic silicon carbide (3C-SiC) has great commercialisation potential as it can be grown epitaxially on inexpensive, large diameter Si wafers. In addition, its manufacturing process is highly compatible with the well-established Si-based process. There have been reports of many devices developed using the 3C-SiC/Si heterostructure, including pressure sensors, strain sensors, and photodetectors [38–40]. LPE-based PSDs utilising the 3C-SiC/Si heterostructure also show great potential with high-sensitivity devices reported [41–46]. However, previous studies on the LPE in 3C-SiC/Si PSD have not considered the effect of an external electrical field across the heterojunction.

In this work, we report for the first time an electric-field-enhanced LPE in 3C-SiC/Si heterojunction and demonstrate it in a highly sensitive PSD. The PSD is fabricated on an n-3C-SiC/p-Si wafer and the position sensing capability of the fabricated devices under external voltage bias is experimentally investigated under the illumination of lasers of different wavelengths (405 nm, 521 nm, and 637 nm) and powers. An excellent position sensitivity as high as 1550 mV/mm is achieved under 5 V reverse bias, which corresponds to a 5-fold enhancement compared to the conventional photovoltaic mode. The generation and transport of photoexcited charge carriers in the heterojunction under reverse bias were thoroughly investigated to gain insights into the phenomenon, working principle and underlying physics of the fabricated devices. Our work demonstrates the potential of the 3C-SiC/Si heterojunction for position sensing and provides a commercially viable platform to develop high-sensitive PSD.

2. Experiment section

Fig. 1a shows the n-3C-SiC/p-Si heterojunction device structure with two aluminium (Al) electrodes on the top and a back Al electrode. The Transmission Electron Microscope (TEM) image of the 3C-SiC/Si heterojunction is shown in Fig. 1b. At the interface, there are visible defects due to the lattice mismatch between the SiC and Si. Figure S1 (Supplementary data) shows the fabrication process of the 3C-SiC/Si heterostructure device. The 380 μm thick Si wafer is cleaned following the standard Radio Corporation of America (RCA) process. From the clean Si wafer, single-crystalline 3C-SiC thin films (90 nm) are grown on both sides of the wafer in the Low-Pressure Chemical Vapor Deposition (LPCVD) process at 1000 $^{\circ}\text{C}$ [47]. To form the back

electrode, the 3C-SiC layer at the back is first removed by Reactive-Ion Etching (RIE). Next, Al is sputtered on the top 3C-SiC layer to make the electrodes. The top Al layer is then spin-coated by a photoresist layer and patterned using a Maskless Aligner (MLA). The electrodes are formed by wet etching. To make the back electrode, Al is deposited on the bare Si by sputtering. Finally, the devices are diced from the wafer.

We use three laser sources (LP405-SF10L, LP520-SF15, LP637-SF70, Thorlabs) with three different wavelengths (405 nm, 521 nm, and 637 nm) to characterise the photoresponse of the heterostructure. The lasers are mounted on a 3-axis stage (PT3, Thorlabs) to control the laser position with a resolution of 25.4 μm (0.001 inches). To observe the laser position on the heterostructure, we use a Digital Microscope (Dino-Lite). The laser spot diameter is monitored by a Beam Profiler (BC106NVIS, Thorlabs) and a spot diameter of approximately 110 μm is maintained. The laser power is measured by a Power Meter (PM100D, Thorlabs) and a Power Sensor (S130C, Thorlabs). The electronic characteristics of the devices are investigated using a Keithley 2450 SourceMeter.

3. Results and discussions

Fig. 2a shows the I - V characteristic of the devices, measured between the lateral electrodes. We observe linear I - V curves for all three electrode spacings, indicating good Ohmic contacts between Al and SiC. The I - V characteristic of the 3C-SiC/Si heterojunction is also measured between the top and bottom electrodes. Fig. 2b shows a logarithmic plot of the I - V curve and an excellent rectification behaviour can be observed. The linear plot of the curve is also shown in the inset.

To characterise the photoresponse, we measure the output LPV of the 3C-SiC/Si heterojunction device between the lateral electrodes when the laser scans from one electrode to the other with different applied reverse biases. Fig. 3a shows the LPV under the zero bias condition. We observe a linear relationship between the output LPV and the laser position, which confirms the position-dependent characteristic of the LPV and indicates the position-sensing applications of the heterostructure. The LPV value reaches the maximum when the laser is at either electrode and it is zero when the laser is at the centre of the electrode spacing (i.e., the distance between electrodes). The LPVs under different applied biases are shown in Fig. 3b. Here, the LPV is measured when the reverse bias from 1 V to 5 V is applied between the top and bottom electrodes. Similar position-dependent behaviour of the LPV can be seen. However, the LPV curves are shifted up, towards the value of the bias voltage. Notably, when the laser is at the centre of the device, an LPV is still generated.

The influence of bias voltage on the position-sensing performance of the heterostructure is further investigated in Fig. 4. To evaluate the position-sensing performance, position sensitivity, which is defined as the change in output voltage divided by the change in position of the laser spot between the two electrodes, is calculated. The sensitivity

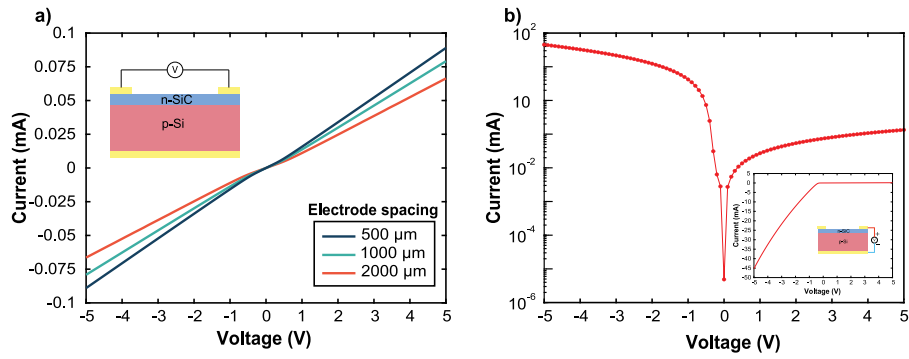


Fig. 2. Current–voltage (I – V) characteristic of the 3C-SiC heterojunction devices, measured between (a) the lateral electrodes, and (b) the top and bottom electrodes.

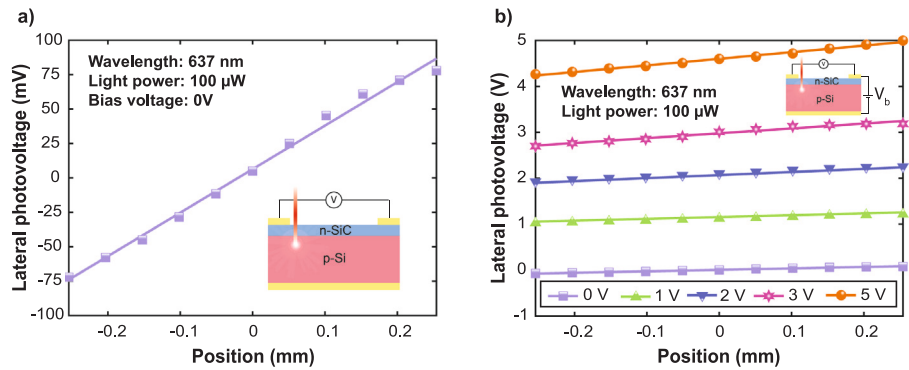


Fig. 3. Dependence of the output lateral photovoltage (LPV) on the laser position when a laser scans from one electrode to the other, measured in the device with the electrode spacing of 500 μm . The measurements are conducted in (a) zero bias, and (b) reverse bias. The incident light has a wavelength of 637 nm and a power of 100 μW .

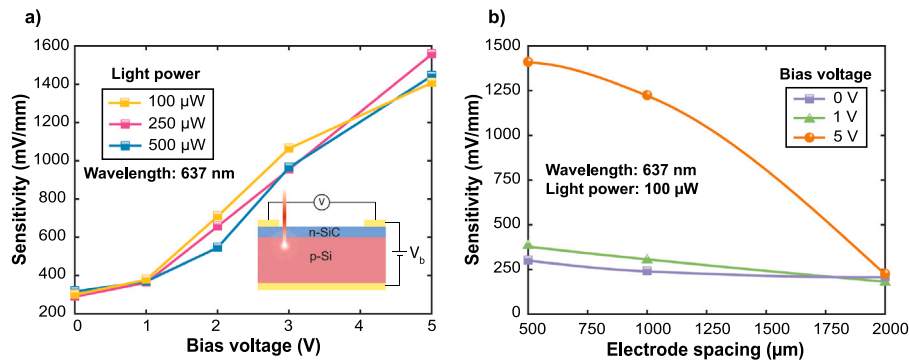


Fig. 4. (a) Dependence of the position sensitivity on the applied reverse bias voltage V_b . (b) Influence of the electrode spacing on the sensitivity at different bias voltages.

of the PSD with increasing bias voltage is shown in Fig. 4a. The sensitivity increases significantly with increasing reverse bias voltage and the enhanced sensitivity follows a linear trend. A sensitivity up to 1550 mV/mm is achieved under a 5 V bias voltage, which is a 5-fold enhancement compared to the zero bias case. This improvement is observed at all measured light powers. Notable works with high position sensitivity were summarised in Table S2, Supplementary data. In addition, the effect of the bias voltage is also investigated on devices with different electrode spacings. At electrode spacings of 500 μm and 1000 μm , the same significant enhancement in sensitivity under reverse bias is seen. However, at the 2000 μm electrode spacing device, the difference in sensitivity at different bias levels is negligible. This can be attributed to the substantial difference between the size of the top electrode and the electrode spacing, with the electrode spacing being ten times larger than the top electrode. Thus, the effect of the electric field on the charge carrier transport is trivial and the sensitivity of the PSD stays almost the same.

The LPE in 3C-SiC/Si heterostructure under applied bias is further investigated at different light powers and wavelengths. Fig. 5a shows the sensitivity of the 500 μm -spacing device under 0 V, 1 V and 5 V bias with increasing incident light power. We observe a sharp increase in sensitivity at all bias conditions when the light power increases. However, when the light power is higher than 250 μW , the sensitivity saturates. Fig. 5b demonstrates the dependence of the sensitivity on the light wavelength. The wavelength-dependence behaviour of the sensitivity under reverse bias is similar to when the device works in conventional photovoltaic mode (i.e., at zero bias). Under the illumination of 637 nm wavelength (250 μW), the sensitivity reaches a maximum value of 1550 mV/mm. The sensitivity decreases as the wavelength decreases and has the lowest value under the 405 nm light source.

To understand the enhanced LPE and working mechanism of the ultrasensitive PSD under reverse bias, we examine the charge carrier generation and transport in the SiC/Si heterojunction. At the SiC/Si

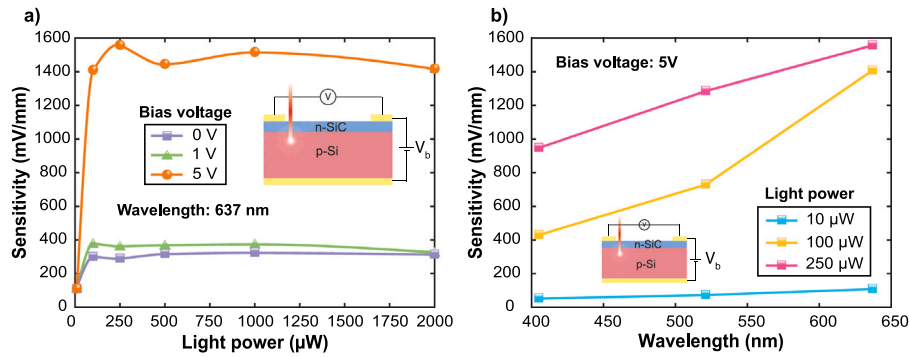


Fig. 5. (a) Dependence of the sensitivity of the PSD on light power, investigated at different bias voltage. (b) Wavelength-dependent position sensitivity when a 5 V reverse bias voltage is applied.

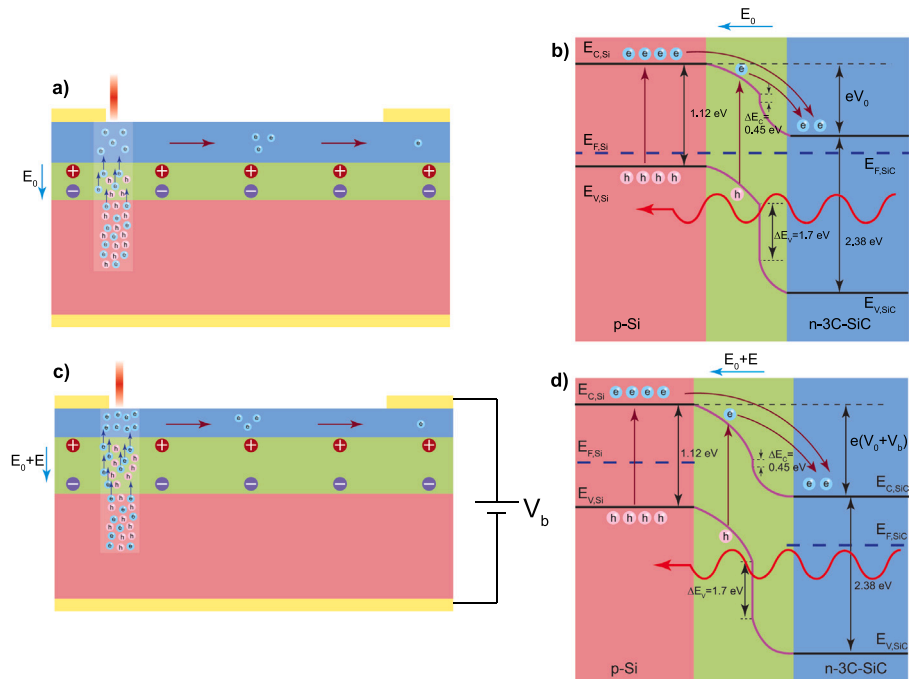


Fig. 6. (a) The photoexcited electron–hole (e–h) pairs transport when the PSD works at zero bias. (b) The energy band diagram of the 3C-SiC/Si heterojunction. (c) The charge carrier’s generation and transport in the heterojunction under reverse bias. (d) The energy band diagram of the heterojunction when a reverse bias is applied.

interface, the highly concentrated electrons in the n-SiC layer diffuse to the p-Si due to the difference in concentration. Similarly, the holes in the p-Si diffuse to the SiC, forming a depletion region at the interface of SiC and Si (Fig. 6a). The diffused electrons leave behind the exposed positive donor ions while the diffused holes left behind the negative acceptor ions. Thus, a built-in electric field is formed across the heterojunction from the positive ions to the negative ions. Under light illumination, charge carriers can be generated in the materials by two main mechanisms: band-to-band transitions (intrinsic) or transitions involving impurities energy levels (extrinsic). Consider the case when a 637 nm light illuminates on the SiC/Si heterojunction. The incident photon energy, in this case, is 1.95 eV, which is lower than the bandgap of 3C-SiC (2.38 eV). Thus, the charge carrier cannot be generated by band-to-band transitions. However, since the 3C-SiC is unintentionally doped, there are donor levels of 0.05 eV in the SiC and photoexcitation can still occur [48]. On the other hand, the photon energy is higher than the bandgap of Si (1.12 eV) and the acceptor levels (0.044 eV) [49]. The incident light is absorbed by the Si and e–h pairs are generated by both intrinsic and extrinsic processes in p-Si. At the incident light wavelength of 521 nm, the photons have higher energy (2.38 eV) thus the band-to-band generation can occur

in 3C-SiC and, thus, a larger number of e–h pairs are generated in the SiC compared to the 637 nm light. In the Si layer, the photon energy of 2.38 eV is much higher than the bandgap of 1.12 eV, the excited electrons have to lose the extra energy to reach a more stable state and thermal equilibrium. The excess energy is lost to lattice vibrations as heat [50,51]. Similarly, at shorter wavelengths (405 nm), even more photons are absorbed in the SiC and more excess energy is lost in the Si. It is important to note that since the thickness of the SiC layer is thin (90 nm) compared to the Si substrate (380 μm), most of the e–h pairs are generated in the Si and the light absorption of the SiC is insignificant [42]. The generation of e–h pairs in the SiC and Si under light illumination is summarised in Table 1, Supplementary data. The generated e–h pairs are separated by the built-in field and drifted in opposite directions. Consider the energy band diagram of the SiC/Si heterojunction in Fig. 6b. The drift corresponds to the photoexcited electrons in the E_C , Si roll down the energy hill, to the SiC region. Similarly, the holes are drifted from SiC to the Si.

When a nonuniform illumination is applied (i.e., a laser beam), the e–h pairs are generated only in the illuminated area and are separated by the built-in voltage at the heterojunction. The electrons move in the opposite direction of the built-in field, towards the n-SiC while holes

move to the p-Si. In the SiC, the electron concentration at the illuminated area is high compared to the unexposed area. Consequently, the electrons diffuse laterally towards electrodes A and B. The redistribution of the photogenerated electrons in the SiC creates a charge carrier gradient between the electrodes, resulting in a lateral LPV. The LPV is linearly proportional to the laser position due to the difference in the diffusion path length from the laser to the electrodes. The LPV between electrodes A and B can be expressed as [17]:

$$V_{AB} = \frac{-2Kn_0}{L_h} (1 - P^{\frac{p_i}{n_0}}) \exp\left(\frac{-L}{L_e}\right)x \quad (1)$$

where $K = (k_B T / q n_T)$ is a proportional coefficient, with n_T is the hole density in the valence band due to temperature fluctuation, T , n_0 is the density of photoexcited electrons, which is defined as $n_0 = (\eta \alpha I \tau / h\nu)$ where η , α , I , τ and $h\nu$ are the quantum efficiency, absorption coefficient, illumination intensity, carrier life time and incident photon energy, respectively. p_i is the power of the incident light. P is the probability that recombination occurs. $2L$ is the distance between electrodes. L_e is the electron's diffusion length and x is the laser position, with $x = 0$ when the laser is at the centre of the electrode spacing.

When a reverse bias voltage is applied between the top and the bottom electrodes, the applied bias voltage drops across the depletion region in the same direction with the built-in voltage, widening the depletion region (Fig. 6c). The negative terminal on p-Si attract more holes in the p-Si to move away from the depletion region, exposing more negative acceptor ions. In the same manner, the positive terminal on n-3C-SiC attracts electrons away from the depletion region thus, the depletion width is widened under reverse bias. The band diagram of the SiC/Si heterojunction under reverse bias is illustrated in Fig. 6d. The Fermi levels $E_{F,Si}$ and $E_{F,SiC}$ are separated by the reverse bias V_b . The potential hill at the junction is higher and becomes steeper due to the large electric field across the heterojunction. When e-h pairs are generated under light illumination, the electrons and holes are separated and drifted by the strong field, resulting in a larger number of electrons migrating to the SiC compared to the case with zero bias. In addition, since the depletion width is greater, more e-h pairs are absorbed in the depletion region, where the majority of the photogeneration takes place. The e-h pairs that are generated outside the depletion region (i.e., in the neutral region) have to diffuse to the region before they can be separated by the electric field and contribute to the output photovoltage. Therefore, by supplying a reverse bias voltage across the heterojunction, the built-in voltage is strengthened and the depletion region is widened, increasing the number of separated e-h pairs, resulting in a great number of photoexcited electrons migrated to the SiC layer. Consequently, the output LPV and position sensitivity are enhanced significantly.

The LPV and sensitivity under reverse bias still depend on the incident light conditions. As discussed above, the light absorption in the SiC/Si heterojunction depends heavily on the compatibility between the light wavelength or photon energy and the material's bandgap. The wavelength dependence characteristic of the 3C-SiC/Si heterojunction mainly depends on the light absorption behaviour of the Si since it was the main absorption layer. When the incident light wavelength is 405 nm, the photon energy of 3.06 eV is larger than the bandgap of both SiC and Si, thus e-h pairs are generated in both layers. However, since the photon energy is much higher than the bandgap of Si (1.12 eV), the excited electrons have to lose the excess energy as heat. In addition, SiC layer thickness (90 nm) is relatively small compared to the Si substrate (380 μm), the contribution of the SiC layer can be considered negligible. With the same light power, at the wavelength of 521 nm, the photon energy is lower (2.38 eV), thus less energy is lost and a larger number of e-h pairs are generated, resulting in a higher position sensitivity. Following the same trend, the light wavelength of 637 nm (1.95 eV) demonstrated the highest position sensitivity among the three wavelengths. We can speculate that the position sensitivity

will continue to increase as the wavelength increases until the incident photon energy matches the bandgap of Si, which corresponds to a wavelength of 1100 nm. At wavelengths larger than this value, the photon energy will be smaller than the bandgap of Si and the number of photo-excited e-h pairs will decrease, resulting in a lower position sensitivity. Furthermore, a number of literature on the LPE using Si as the main absorption layer also reported optimum position sensitivity values at wavelengths in the near-infrared range. In addition, the light power also has influences on the sensitivity. Intuitively, the position sensitivity increases with increasing light power due to the higher number of incident photons coming onto the material surface. However, the sensitivity saturates and does not increase further at high power ranges (250 μW). As the number of photoexcited e-h pairs increases with increasing light power, the recombination rate also increases [52,53]. Eventually, the recombination process becomes dominant, resulting in the saturation of sensitivity at high light power.

4. Conclusion

In conclusion, we investigated the enhanced LPE in 3C-SiC/Si heterojunction and its position sensing capability under an applied electric field. The output LPV and position sensitivity were measured under the illumination of lasers when a reverse bias was applied across the heterojunction. The heterostructure exhibits an excellent linear relationship between the laser position and the output LPV. The sensitivity increases significantly as the reverse bias voltage increase from 1 V to 5 V and reaches a maximum value of 1550 mV/mm. To explain this 5-fold improvement in sensitivity, the charge carrier generation and transport in the heterojunction is investigated using the energy band diagram. The giant sensitivity can be attributed to the widened depletion region, resulting in a larger number of photons absorbed in this region, thus strengthening the separation process of the photogenerated e-h pairs. The position-sensing performance is also investigated in devices with different electrode spacing and under different light wavelengths and powers. At large electrode spacing of 2000 μm , the sensing performance of the heterojunction PSD shows almost no change at zero bias and reverse bias. This could be attributed to the large size discrepancy between the electrode spacing and the electrode width, which minimise the effect of the reverse bias on the heterojunction. The position sensitivity reaches the highest value under the illumination of the 637 nm laser, which corresponds to the absorption band of Si. The PSD also shows better performance under high-power illumination; however, the position sensitivity saturates when the light power reaches a certain level. These dependencies of the position sensitivity on the light conditions of the PSD under reverse bias are consistent with the zero bias case. The findings in this work verify the ultra-sensitive position sensing performance of the 3C-SiC/Si heterojunction under an electric field, demonstrating the commercial potential of the heterojunction in developing optoelectronic sensors. To further enhance the performance of the 3C-SiC/Si PSD, the following future research should be conducted. First, the influence of other external modulations on the LPE can be investigated. For instance, the LPE has been reported to be greatly affected by the magnetic field and thermal energy in different materials and structures. Investigating the effect of these stimulations on the LPE can provide further insight into the physics of the LPE in 3C-SiC/Si and potentially enhance the LPE. Secondly, by modifying the surface morphology of the SiC layer, the optoelectronic properties of the heterostructure can be improved and enhanced. For instance, nanopillars, and nanopyramids structures have been reported to increase the light-trapping capability of the structure. Finally, by combining the 3C-SiC/Si heterostructure with other photosensitive materials, especially, 2D materials such as perovskites to create multi-junction structures, interesting optoelectronic phenomena can be observed and the light-harvesting capability may be enhanced.

CRedit authorship contribution statement

Tuan-Hung Nguyen: Conceptualization, Methodology, Formal analysis, Investigation, Data curation, Writing – original draft, Writing – review & editing, Visualization. **Trung-Hieu Vu:** Writing – review & editing. **Tuan Anh Pham:** Resources, Writing – review & editing. **Dinh Gia Ninh:** Writing – review & editing. **Cong Thanh Nguyen:** Writing – review & editing. **Hong-Quan Nguyen:** Writing – review & editing. **Braiden Tong:** Writing – review & editing. **Dang D.H. Tran:** Data curation, Writing – review & editing. **Erik W. Streed:** Resources. **Van Thanh Dau:** Supervision, Writing – review & editing. **Nam-Trung Nguyen:** Resources, Supervision, Writing – review & editing. **Dzung Viet Dao:** Resources, Supervision, Writing – review & editing, Funding acquisition, Validation.

Declaration of competing interest

The authors declare that they have no known competing financial interests or personal relationships that could have appeared to influence the work reported in this paper.

Data availability

Data will be made available on request

Acknowledgements

This work was performed in part at the Queensland node of the Australian National Fabrication Facility. A company established under the National Collaborative Research Infrastructure Strategy to provide nano and microfabrication facilities for Australia's researchers. The 3C-SiC material was developed and supplied by Leonie Hold and Alan Iacopi. The epitaxial SiC deposition was developed as part of Griffith University Joint Development Agreement with SPT Microtechnology, the manufacturer of the Epiflx production reactor. This work has been partially supported by Australian Research Council Discovery Project DP220101252.

Appendix A. Supplementary data

Supplementary material related to this article can be found online at <https://doi.org/10.1016/j.sna.2023.114746>.

References

- [1] X. Du, W. Tian, J. Pan, B. Hui, J. Sun, K. Zhang, Y. Xia, Piezo-phototronic effect promoted carrier separation in coaxial p-n junctions for self-powered photodetector, *Nano Energy* 92 (2022) 106694.
- [2] F. Gao, H. Chen, W. Feng, Y. Hu, H. Shang, B. Xu, J. Zhang, C. Xu, P. Hu, High-performance van Der Waals metal-insulator-semiconductor photodetector optimized with valence band matching, *Adv. Funct. Mater.* 31 (35) (2021) 2104359.
- [3] H. Wang, L. Li, J. Ma, J. Li, D. Li, 2D perovskite narrowband photodetector arrays, *J. Mater. Chem. C* 9 (34) (2021) 11085–11090.
- [4] D. Wu, J. Guo, C. Wang, X. Ren, Y. Chen, P. Lin, L. Zeng, Z. Shi, X.J. Li, C.-X. Shan, Ultrabroadband and high-detectivity photodetector based on WS_2/Ge heterojunction through defect engineering and interface passivation, *ACS Nano* 15 (6) (2021) 10119–10129.
- [5] K. Liu, W. Wang, Y. Yu, X. Hou, Y. Liu, W. Chen, X. Wang, J. Lu, Z. Ni, Graphene-based infrared position-sensitive detector for precise measurements and high-speed trajectory tracking, *Nano Lett.* 19 (11) (2019) 8132–8137.
- [6] Y.-C. Wang, C.-S. Huang, Flexible linear and angular displacement sensor based on a gradient guided-mode resonance filter, *IEEE Sens. J.* 18 (24) (2018) 9925–9930.
- [7] U. Wijesinghe, A. Dey, W. Krenik, H. Edwards, A. Marshall, M. Lee, Microelectronic angular displacement sensor with near hemispherical linear field-of-view, *IEEE Sens. J.* 22 (5) (2022) 4051–4056.
- [8] K. Liu, D. Wan, W. Wang, C. Fei, T. Zhou, D. Guo, L. Bai, Y. Li, Z. Ni, J. Lu, A time-division position-sensitive detector image system for high-speed multitarget trajectory tracking, *Adv. Mater.* 34 (47) (2022) e2206638.

- [9] C.H. Huang, S.W. Tan, H. Lo, C. Lo, C.W. Chen, W.S. Lour, High-sensitivity position-sensitive detectors to low-power light spots, *Sensors Actuators A* 347 (2022).
- [10] M. Grajower, B. Desiatov, N. Mazurski, U. Levy, Integrated on-chip silicon plasmonic four quadrant detector for near infrared light, *Appl. Phys. Lett.* 113 (14) (2018) 143103.
- [11] Y. Yifat, J. Parker, T.-S. Deng, S.K. Gray, S.A. Rice, N.F. Scherer, Facile measurement of the rotation of a single optically trapped nanoparticle using the diagonal ratio of a quadrant photodiode, *ACS Photonics* 8 (11) (2021) 3162–3172.
- [12] A. Dong, H. Wang, Lateral photovoltaic effect and photo-induced resistance effect in nanoscale metal-semiconductor systems, *Ann. Phys.* 531 (7) (2019) 1800440.
- [13] J.T. Wallmark, A new semiconductor photocell using lateral photoeffect, *Proc. IRE* 45 (4) (1957) 474–483.
- [14] S. Qiao, B. Liang, J. Liu, G. Fu, S. Wang, Lateral photovoltaic effect based on novel materials and external modulations, *J. Phys. D: Appl. Phys.* 54 (15) (2021).
- [15] R. Cong, S. Qiao, J. Liu, J. Mi, W. Yu, B. Liang, G. Fu, C. Pan, S. Wang, Ultrahigh, Ultrafast, And self-powered visible-near-infrared optical position-sensitive detector based on a CVD-prepared vertically standing few-layer MoS_2/Si heterojunction, *Adv. Sci.* 5 (2) (2018) 1700502.
- [16] L. Hao, H. Xu, S. Dong, Y. Du, L. Luo, C. Zhang, H. Liu, Y. Wu, Y. Liu, $SnSe/SiO_2/Si$ heterostructures for ultrahigh-sensitivity and broadband optical position sensitive detectors, *IEEE Electron Device Lett.* 40 (1) (2019) 55–58.
- [17] Y. Zhang, Y. Zhang, T. Yao, C. Hu, Y. Sui, X. Wang, Ultrahigh position sensitivity and fast optical relaxation time of lateral photovoltaic effect in $Sb_2Se_3/p-Si$ junctions, *Opt. Express* 26 (26) (2018) 34214–34223.
- [18] X. Zhao, L. Zhang, Q. Gai, C. Hu, X. Wang, High-performance position-sensitive detector based on the lateral photovoltaic effect in $MoSe_2/p-Si$ junctions, *Appl. Opt.* 58 (19) (2019) 5200–5205.
- [19] Y. Cao, Z. Zhao, P. Bao, Z. Gan, H. Wang, Lateral photovoltaic effect in silk-protein-based nanocomposite structure for physically transient position-sensitive detectors, *Phys. Rev. A* 15 (5) (2021).
- [20] J. Ma, M. Chen, S. Qiao, J. Chang, G. Fu, S. Wang, Photovoltaic-pyroelectric coupled effect in Ag_2Se/Si heterojunction for broad-band, ultrafast, self-powered, position-sensitive detectors, *ACS Photonics* 9 (6) (2022) 2160–2169.
- [21] W. Wang, K. Liu, J. Jiang, R. Du, L. Sun, W. Chen, J. Lu, Z. Ni, Ultrasensitive graphene-Si position-sensitive detector for motion tracking, *InfoMat* 2 (4) (2020) 761–768.
- [22] M. Zhu, K. Meng, C. Xu, J. Zhang, G. Ni, Lateral photovoltaic effect in ITO/PEDOT:PSS/MEH-PPV/PCBM/Al organic photovoltaic cells, *Organic Electronics* 78 (2020).
- [23] X. Dong, D. Zheng, J. Lu, Y. Niu, H. Wang, Efficient hot electron extraction in $Ag-Cu/TiO_2$ for high performance lateral photovoltaic effect, *IEEE Electron Device Lett.* 42 (10) (2021) 1500–1503.
- [24] N. Ganesh, K. Schutt, P.K. Nayak, H.J. Snaith, K.S. Narayan, 2D position-sensitive hybrid-perovskite detectors, *ACS Appl. Mater. Interfaces* 13 (45) (2021) 54527–54535.
- [25] Z. Liang, J. Liu, J. Ma, Z. Li, S. Wang, S. Qiao, Multifunctional high-performance position sensitive detector based on a Sb_2Se_3 -nanorod/CdS core-shell heterojunction, *Opt. Express* 30 (22) (2022) 40491–40504.
- [26] X. Zhao, R. Wang, P. Bao, Y. Niu, D. Zheng, Z. Zhao, N. Su, C. Hu, S. Hu, Y. Wang, H. Wang, Large near-infrared lateral photovoltaic effect in an organic egg albumin/Si structure, *Opt. Lett.* 47 (16) (2022).
- [27] D. Zheng, X. Dong, J. Lu, Y. Niu, H. Wang, High-sensitivity infrared photoelectric detection based on WSe_2/Si structure tuned by ferroelectrics, *Small* 18 (7) (2022) e2105188.
- [28] J. Liu, X. Dong, J. Chen, Z. Zhang, S. Wang, S. Qiao high-sensitivity flexible position sensing in a $Cu(In, Ga)Se_2$ multi-layer heterojunction tuned by piezo-pyroelectric effect, *Nano Energy* 109 (2023) 108254.
- [29] T.-H. Nguyen, A.R.M. Faisal, T.A. Pham, T.-H. Vu, H.-Q. Nguyen, E.W. Streed, J. Fastier-Wooller, P.G. Duran, P. Tanner, V.T. Dau, N.-T. Nguyen, D.V. Dao, Effect of 3c-sic layer thickness on lateral photovoltaic effect in 3C-SiC/Si heterojunction, *IEEE Sensors J.* (2023).
- [30] D. Zheng, X. Dong, J. Lu, Y. Niu, H. Wang, Ultrafast and hypersensitized detection based on van Der Waals connection in two-dimensional WSe_2/Si structure, *Appl. Surface Sci.* 574 (2022).
- [31] L.Z. Hao, Y.J. Liu, Z.D. Han, Z.J. Xu, J. Zhu, Giant lateral photovoltaic effect in $MoS_2/SiO_2/Si$ P-I-N junction, *J. Alloys Compd.* 735 (2018) 88–97.
- [32] C. Hu, X. Wang, P. Miao, L. Zhang, B. Song, W. Liu, Z. Lv, Y. Zhang, Y. Sui, J. Tang, Y. Yang, B. Song, P. Xu, Origin of the ultrafast response of the lateral photovoltaic effect in amorphous MoS_2/Si junctions, *ACS Appl. Mater. Interfaces* 9 (21) (2017) 18362–18368.
- [33] S. Qiao, J. Liu, G. Fu, S. Wang, K. Ren, C. Pan, Laser-induced photoresistance effect in Si-based vertical standing MoS_2 nanoplate heterojunctions for self-powered high performance broadband photodetection, *J. Mater. Chem. C* 7 (34) (2019) 10642–10651.
- [34] W. Wang, Z. Yan, J. Zhang, J. Lu, H. Qin, Z. Ni, High-performance position-sensitive detector based on graphene-silicon heterojunction, *Optica* 5 (1) (2018).

- [35] T. Xu, Y. Han, L. Lin, J. Xu, Q. Fu, H. He, B. Song, Q. Gai, X. Wang, Self-power position-sensitive detector with fast optical relaxation time and large position sensitivity basing on the lateral photovoltaic effect in tin diselenide films, *J. Alloys Compd.* 790 (2019) 941–946.
- [36] H.-P. Phan, D.V. Dao, K. Nakamura, S. Dimitrijevic, N.-T. Nguyen, The piezoresistive effect of SiC for MEMS sensors at high temperatures: A review, *J. Microelectromech. Syst.* 24 (6) (2015) 1663–1677.
- [37] X. She, A.Q. Huang, L. Ó., B. Ozpineci, Review of silicon carbide power devices and their applications, *IEEE Trans. Ind. Electron.* 64 (10) (2017) 8193–8205.
- [38] A.R. Md Foisal, T. Dinh, V.T. Nguyen, P. Tanner, H.-P. Phan, T.-K. Nguyen, B. Haylock, E.W. Streed, M. Lobino, D.V. Dao, Self-powered broadband (UV-NIR) photodetector based on 3C-SiC/Si heterojunction, *IEEE Trans. Electron Devices* 66 (4) (2019) 1804–1809.
- [39] T. Nguyen, T. Dinh, V.T. Dau, H. Nguyen, T.H. Vu, C.-D. Tran, P. Song, J. Bell, N.-T. Nguyen, D.V. Dao, The concept of light-harvesting, self-powered mechanical sensors using a monolithic structure, *Nano Energy* 96 (2022) 107030.
- [40] B. Tong, T.-H. Nguyen, H.-Q. Nguyen, T.-K. Nguyen, T. Nguyen, T. Dinh, N.V.K. Thanh, T.H. Ly, N.C. Cuong, H.B. Cuong, Highly sensitive and robust 3C-SiC/Si pressure sensor with stress amplification structure, *Mater. Des.* 224 (2022) 111297.
- [41] A.R.M. Foisal, T. Nguyen, T. Dinh, T.K. Nguyen, P. Tanner, E.W. Streed, D.V. Dao, 3C-SiC/Si heterostructure: An excellent platform for position-sensitive detectors based on photovoltaic effect, *ACS Appl. Mater. Interfaces* 11 (43) (2019) 40980–40987.
- [42] A.R.M. Foisal, A. Qamar, T. Nguyen, T. Dinh, H.P. Phan, H. Nguyen, P.G. Duran, E.W. Streed, D.V. Dao, Ultra-sensitive self-powered position-sensitive detector based on horizontally-aligned double 3C-SiC/Si heterostructures, *Nano Energy* 79 (2021).
- [43] H. Nguyen, A. Riduan Md Foisal, T. Nguyen, T. Dinh, E.W. Streed, N.-T. Nguyen, D. Viet Dao, Effects of photogenerated-hole diffusion on 3C-SiC/Si heterostructure optoelectronic position-sensitive detector, *J. Phys. D: Appl. Phys.* 54 (26) (2021).
- [44] T.H. Nguyen, T. Nguyen, A.R.M. Foisal, T. Dinh, H.Q. Nguyen, E.W. Streed, T.H. Vu, P. Tanner, V.T. Dau, N.T. Nguyen, D.V. Dao, Generation of a charge carrier gradient in a 3C-SiC/Si heterojunction with asymmetric configuration, *ACS Appl. Mater. Interfaces* 13 (46) (2021) 55329–55338.
- [45] T.-H. Nguyen, T. Nguyen, A.R.M. Foisal, T.A. Pham, T. Dinh, H.-Q. Nguyen, E.W. Streed, T.-H. Vu, J. Fastier-Wooller, P.G. Duran, V.T. Dau, N.-T. Nguyen, D.V. Dao, Ultrasensitive self-powered position-sensitive detector based on n-3C-SiC/p-Si heterojunctions, *ACS Appl. Electron. Mater.* 4 (2) (2022) 768–775.
- [46] T.-H. Nguyen, T.A. Pham, T.-H. Vu, H.-Q. Nguyen, P.G. Duran, E.W. Streed, J.W. Fastier-Wooller, V.T. Dau, N.-T. Nguyen, D.V. Dao, Giant lateral photovoltage in a SiC/Si heterojunction with a micro free-standing SiC serpentine beam, *ACS Appl. Energy Mater.* 5 (8) (2022) 9830–9836.
- [47] L. Wang, S. Dimitrijevic, J. Han, A. Iacopi, L. Hold, P. Tanner, H.B. Harrison, Growth of 3C-SiC on 150-nm Si(100) substrates by alternating supply epitaxy at 1000 °C, *Thin Solid Films* 519 (19) (2011) 6443–6446.
- [48] M. Yamanaka, H. Daimon, E. Sakuma, S. Misawa, S. Yoshida, Temperature dependence of electrical properties of n-and p-type 3C-SiC, *J. Appl. Phys.* 61 (2) (1987) 599–603.
- [49] S.M. Sze, K.K. Ng, *Physics of Semiconductor Devices*, John Wiley & Sons, 2006.
- [50] T. Ibn-Mohammed, S.C.L. Koh, I.M. Reaney, A. Acquaye, G. Schileo, K.B. Mustapha, R. Greenough, Perovskite solar cells: An integrated hybrid lifecycle assessment and review in comparison with other photovoltaic technologies, *Renew. Sustain. Energy Rev.* 80 (2017) 1321–1344.
- [51] A. Shang, X. Li, Photovoltaic devices: Opto-electro-thermal physics and modeling, *Adv. Mater.* 29 (8) (2017) 1603492.
- [52] J.-J. Huang, H.-C. Kuo, S.-C. Shen, *Nitride Semiconductor Light-Emitting Diodes (LEDs): Materials, Technologies, and Applications*, Woodhead Publishing, 2017.
- [53] T. Tayagaki, S. Fukatsu, Y. Kanemitsu, Photoluminescence dynamics and reduced auger recombination in $\text{Si}_{1-x}\text{Ge}_x/\text{Si}$ superlattices under high-density photoexcitation, *Phys. Rev. B* 79 (4) (2009) 041301.



Trung-Hieu Vu received the B.S degree in Mechanical Engineering from Griffith University, Australia in 2020. He is currently working on his Ph.D. at Griffith in fabrication of nanoparticles and nanofibres via electro-spray/electrospinning. Electrohydrodynamics and microfluidics are his main research subjects.



Tuan Anh Pham is currently working as a research staff in Michigan State University, USA. Before relocating to Michigan, Dr. Pham worked as a researcher in various research institutes, including University of Groningen (the Netherlands, 2011 to 2016), University of Erlangen–Nuremberg (Germany, 2016 to 2017), Institute for Basic Science (South Korea, 2017 to 2019) and Nanyang Technological University (Singapore, 2019 to 2020) and Griffith University (2020–2022). He published 41 scientific papers, many of them in leading journals. His current research interest focuses on semiconductor thin film, low-dimensional materials, surface characterisations and device fabrications for electronic/photonic applications.



Dinh Gia Ninh obtained his bachelor's degree from Hanoi University of Science and Technology, in 2012. His current research interests include Materials and Structures, Soft Robotics, MEMS and NEMS, Optics, and AI and Machine Learning.



Cong Thanh Nguyen is currently a Research Fellow in the School of Engineering and Built Environment, Griffith University, Australia. He received his Ph.D. in Mechanical and Mechatronics Engineering from University of Technology Sydney, in 2021. His research interests include micro-electro-mechanical systems (MEMS), silicon carbide MEMS for harsh environments, physics of semiconductors, self-powered and energy-harvesting sensors, and composite materials and structures.



Hong-Quan Nguyen received his Ph.D. degree from Griffith University, Australia in 2021. He then served as a Post-doctoral Research Fellow from 2021 to 2022. From 2022, he joined Hanoi University of Science and Technology, Vietnam, where he has been teaching in Mechatronics and Mechanical Engineering. His current research interests include advanced manufacturing, MEMS sensors and actuators, transducers for harsh environments.



Braiden Tong received the B.S degree in Mechanical Engineering from Griffith University, Australia in 2021. He is currently working on his Ph.D. at Queensland Micro- and Nanotechnology Centre, Griffith University, Australia on the use of wide bandgap semiconductors to develop physical sensors. His main research interests are silicon carbide and gallium nitride MEMS sensors for harsh environments.



Dang D.H. Tran received the B.E. in Automation Technology from HCMC University of Technology and Education, Vietnam, in 2014, and M.Sc. degree in Mechatronic and Sensors Systems Technology from Karlsruhe University of Applied Sciences, Germany, in 2018. From 2018 to 2022, he worked in a top semiconductor company in Japan as a sensor products specialist before pursuing his Ph.D. degree at Queensland Micro- and Nanotechnology Centre, Griffith University, QLD, Australia, from 2022, researching on silicon carbide (SiC) material for sensor applications. His main research interest includes MEMS Sensors, silicon carbide MEMS/NEMS, and sensors systems.



Tuan-Hung Nguyen received his Ph.D from Queensland Micro- and Nanotechnology Centre, Griffith University, Australia. He received his M.S. and B.E. degrees in mechanical engineering from Seoul National University of Science and Technology, Korea and Hanoi University of Science and Technology, Vietnam, respectively. His research interests are optoelectronic MEMS sensors, silicon carbide MEMS/NEMS, and optomechatronic systems. He was awarded the competitive Griffith University Postgraduate Research Scholarship (GUPRS) and Griffith University International Postgraduate Research Scholarship (GUIPRS). His works were featured several times on the covers of prestigious journals.



Erik Streed (Associate Professor), is a physicist in Griffith University's School of Environment and Science, the Deputy Director of the Centre for Quantum Dynamics, and a Research Leader in the Institute for Glycomics. He is best known for his pioneering work in integrating diffractive optics with trapped ions, which lead to the first imaging of a single atom's shadow. A graduate of Caltech (B.Sc. Physics) and MIT (Ph.D. Physics), he completed his graduate work in Bose–Einstein condensate in the group of Wolfgang Ketterle (Physics Nobel 2001).



Dr Van Thanh Dau received the B.S. degree in aerospace engineering from Hochiminh City University of Technology, Vietnam, in 2002, and the M.S. and Ph.D. degrees in micromechatronics from Ritsumeikan University, Japan, in 2004 and 2007, respectively. From 2007 to 2009, he was a Postdoctoral Fellow with Japan Society for the Promotion of Science (JSPS). From 2010 to 2018, he had worked for a start-up in England and leading companies in Japan before joining Griffith University in 2019. He has published 150+ papers and 23 inventions (8 US patents) in the field of MEMS, electrohydrodynamics and nano printing. His inventions have led to 5+ commercial products. He is a senior member of IEEE and currently leads a team of 7 Ph.D. students at the School of Engineering and Built Environment, Griffith University. His research focuses on MEMS sensors and actuators, electrohydrodynamics, flexible electronics, aerosol and respiratory medical device.



Nam-Trung Nguyen received his Dip-Ing, Dr Ing and Dr Ing Habil degrees from Chemnitz University of Technology, Germany, in 1993, 1997 and 2004, respectively. In 1998, he was a postdoctoral research engineer in the Berkeley Sensor and Actuator Center (University of California at Berkeley, USA). He is a Fellow of ASME and a Senior Member of IEEE. Nguyen's research is focused on microfluidics, nanofluidics, micro/nanomachining technologies, micro/nanoscale science, and instrumentation for biomedical applications. He published over 500 journal papers and filed 8 patents, of which 3 were granted. Among the books he has written, the first and second and third editions of the bestseller "Fundamentals and Applications of Microfluidics" were published in 2002, 2006 and 2019, respectively.



Dzung Viet Dao received his Ph.D. degree in Micro Electro Mechanical Systems (MEMS) from Ritsumeikan University, Japan in 2003. He served as a Postdoctoral Research Fellow from 2003 to 2006, Lecturer from 2006 to 2007, and Chair Professor from 2007 to 2011, all at Ritsumeikan University, Japan. From 2011 Dr Dao joined Griffith University, Australia, as a Professor in the School of Engineering and Built Environment, where he is currently teaching Mechatronics and Mechanical Engineering. His current research interests include advanced sensing effects in nano materials, MEMS sensors & actuators, sensors for harsh environment, and wireless sensor network.